International Journal of Pharmaceutics 403 (2011) 207–218

Contents lists available at ScienceDirect

International Journal of Pharmaceutics

journal homepage: www.elsevier.com/locate/ijpharm

Pharmaceutical Nanotechnology

Cellular uptake and degradation behaviour of biodegradable poly(ethylene glycol-graft-methyl methacrylate) nanoparticles crosslinked with dimethacryloyl hydroxylamine

Stefan Scheler*, Martina Kitzan, Alfred Fahr

Friedrich Schiller University of Jena, Department of Pharmaceutical Technology, Lessingstr. 8, 07743 Jena, Germany

ARTICLE INFO

Article history:
Received 4 August 2010
Received in revised form 11 October 2010
Accepted 13 October 2010
Available online 20 October 2010

Keywords:
Nanoparticle
Biodegradation
Cross-linking
Polyethylene oxide
Cell culture
Fibroblast

ABSTRACT

Crosslinked polymers with hydrolytically cleavable linkages are highly interesting materials for the design of biodegradable drug carriers. The aim of this study was to investigate if nanoparticles made of such polymers have the potential to be used also for intracellular drug delivery. PEGylated nanoparticles were prepared by copolymerization of methacrylic acid esters and N,O-dimethacryloylhydroxylamine (DMHA). The particles were stable at pH 5.0. At pH 7.4 and 9.0 the degradation covered a time span of about 14 days, following first-order kinetics with higher crosslinked particles degrading slower. Cellular particle uptake and cytotoxicity were tested with L929 mouse fibroblasts. The particle uptake rate was found to correlate linearly with the surface charge and to increase as the zeta potential becomes less negative. Coating of the particle surface with polysorbate 80 drops the internalization rate close to zero and the charge dependence disappears. This indicates the existence of a second effect apart from surface charge. A similar pattern of correlation with zeta potential and coating was also found for the degree of membrane damage while there was no effect of polysorbate on the cell metabolism which increased as the negative charge decreased. It is discussed whether exocytotic processes may explain this behaviour.

1. Introduction

Nanoparticulate carrier systems provide a promising technology for intracellular drug delivery. Although nanoparticles based on biodegradable polymers have gained increasing attention for this purpose only a limited number of suitable materials has been studied so far. In general three distinct mechanisms of biodegradation can be identified (Rosen et al., 1988): (i) cleavage of the polymer backbone, (ii) conversion of polymer side chains into polar or charged moieties thus increasing the solubility, and (iii) cleavage of crosslinks between water-soluble polymer chains. The first mechanism is the underlying principle of biodegradable polyanhydrides and polyesters e.g. poly(lactic acid) (PLA) and the widely used copolymers of lactic and glycolic acid (PLGA). Biodegradation of poly(butyl cyanoacrylate) (PBCA) or poly(hexadecyl cyanoacrylate) follows the second principle. By cleaving the alkyl ester side chains and thereby creating free carboxylic groups the polymer becomes water soluble. Rarely employed and poorly investigated is the third type of materials: crosslinked polymers with cleavable linkages. Early developments in this field were N-(2-hydroxypropyl methacrylamide) polymers crosslinked by enzymatically degradable oligopeptide sequences (Ulbrich et al., 1982; Šubr et al., 1990). Their disadvantage is that, though they are rapidly cleaved in vitro in the presence of hydrolytic enzymes, they degrade only slowly after implantation in vivo. A non-enzymatically cleavable crosslinked network can be obtained by copolymerization of acrylic acid derivatives with the crosslinking agent N,O-dimethacryloyl hydroxylamine (DMHA) (Ulbrich et al., 1993; Horák and Chaykivskyy, 2002; Horák and Kroupová, 2004; Přádný et al., 2006; Syková et al., 2006; Chivukula et al., 2006; Smith et al., 2010). The structure of these polymers consists of a three-dimensional network of polyacrylate chains interconnected via dicarbonyl hydroxylamine (–COONHCO–) linkages, susceptible to hydrolytic cleavage. Nanoparticles consisting of DMHA-crosslinked poly(ethylene glycol-graft-methyl methacrylate) diblock copolymers were shown by in vitro tests to be applicable as sustained release drug carriers (Yin et al., 2002). In recent years nanoparticles gained increasing attention not only as intravenously injectable carrier systems but also as vehicles for intracellular drug target-

Abbreviations: AIBN, 2,2′-azobisisobutyronitrile; DiI, 1,1′-dioctadecyl-3,3,3′,3′-tetramethylindocarbocyanine perchlorate; DMHA, N,O-dimethacryloyl hydroxylamine; EGDMA, ethyleneglycol dimethacrylate; MAA, methacrylic acid; MMA, methyl methacrylate; PEO-MA, poly(ethylene glycol) methyl ether methacrylate; PVA, poly(vinyl alcohol).

* Corresponding author at: Sandoz GmbH, Sandoz Development Center Austria, Biochemiestr. 10, 6250 Kundl, Austria.
Tel.: +43 5338 200 2793; fax: +43 5338 200 3238.
E-mail addresses: stefan.scheler@sandoz.com, stefan.scheler@t-online.de (S. Scheler).

0378-5173/$ – see front matter © 2010 Elsevier B.V. All rights reserved.
doi:10.1016/j.ijpharm.2010.10.019

ing. Many previous studies have addressed the cellular uptake of PLA (Bejjani et al., 2005; De Jaeghere et al., 2000; Harush-Frenkel et al., 2007; Sun et al., 2004), PLGA (Sahoo et al., 2002; Nakano et al., 2007; Panyam and Labhasetwar, 2003; Sahoo and Labhasetwar, 2005) or poly(cyanacrylate) nanoparticles (Kim et al., 2007; Ramge et al., 2000). The interaction of DMHA-crosslinked poly(ethylene glycol-graft-methyl methacrylate) nanoparticles with cells was not investigated so far. It is well known that the cellular uptake of polymer nanoparticles is strongly influenced by the monomer composition and also the surface charge plays a pivotal role. The latter is often determined by the functional groups of the polymer and thus can change when linkages are cleaved. For this reason this study was performed to elucidate the cellular uptake of this relatively novel type of nanoparticles and to understand their behaviour with respect to physicochemical properties and cytotoxicity. PEGylation of nanoparticles is often applied to enhance their dispersibility and to reduce phagocytosis by the reticuloendothelial system. PEGylated nanoparticles were also shown to penetrate the blood–brain-barrier to a larger extent than non-coated particles (Calvo et al., 2001). Based on a method described by Yin et al. (2002) PEGylated nanoparticles were synthesized by crosslinking copolymerization from methyl methacrylate (MMA), DMHA and methoxypolyethylene glycol methacrylate (PEO-MA) (Fig. 1). Three hydrolysable formulations with different degrees of cross-

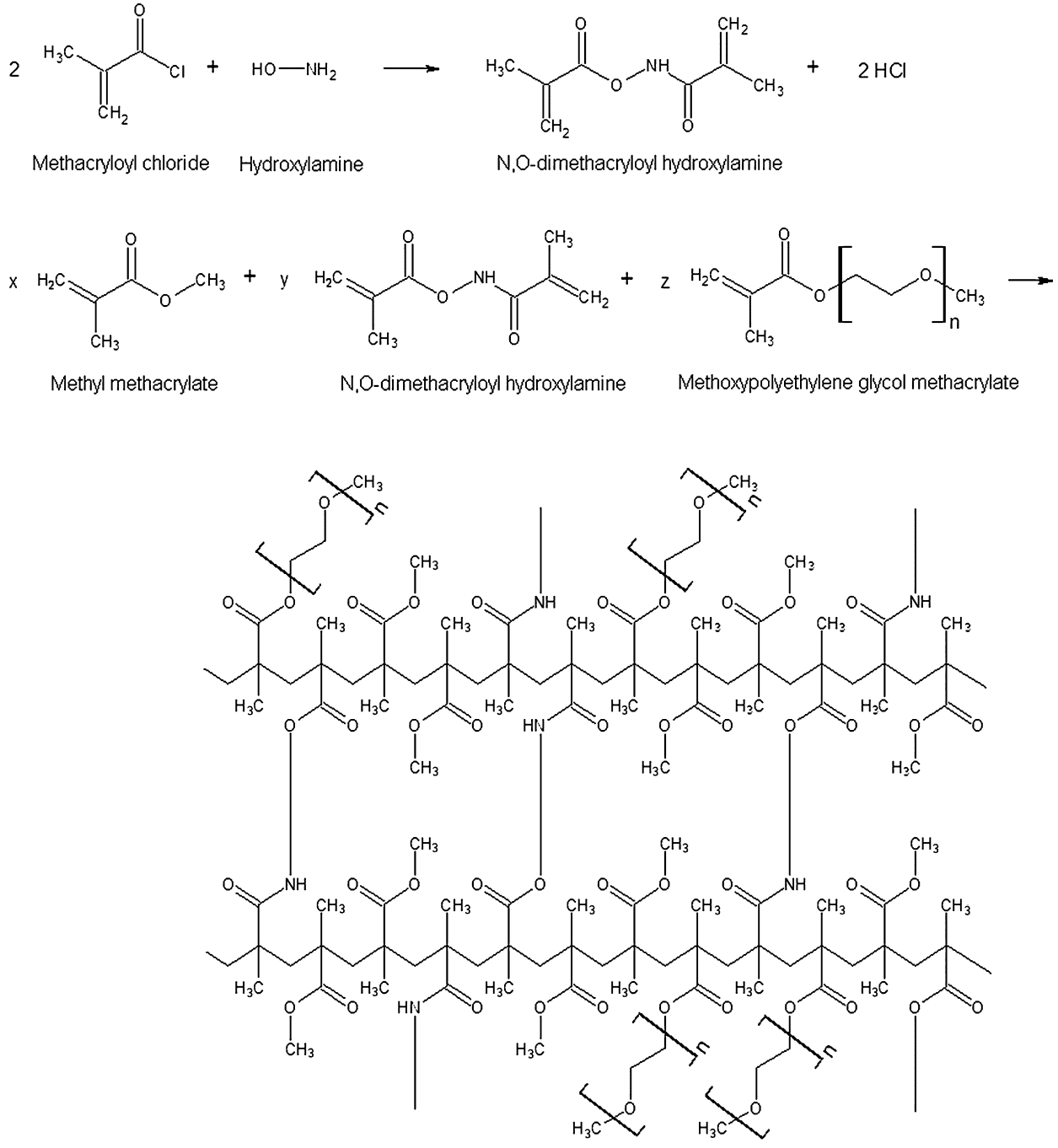

Fig. 1. Synthesis of DMHA-crosslinked poly(ethylene glycol-graft-methyl methacrylate).

linking were compared to a non-cleavable formulation crosslinked with ethyleneglycol dimethacrylate (EGDMA) and to an EGDMA-crosslinked formulation copolymerized with an additional amount of methacrylic acid (MAA). The degradation of these particles was studied in vitro and for the first time the cellular uptake of nanoparticles made of DMHA-crosslinked polymers was investigated. The tests were performed with the mouse fibroblast cell line L929.

2. Materials and methods

2.1. Materials and chemicals

Methyl methacrylate (purum, ≥99.0%), methacryloyl chloride (≥97.0%, stabilized), hydroxylamine hydrochloride (puriss. p.a., for ASS ≥99.0%), poly(ethylene glycol) methyl ether methacrylate (PEO-MA) (av. M_n ~1100), poly(vinyl alcohol) (PVA) (av. M_W 30,000–70,000, 87–90% hydrolyzed), 1,1′-dioctadecyl-3,3,3′,3′-tetramethylindocarbocyanine perchlorate (97%) (DiI), and trypan blue solution 0.4% were purchased from Sigma–Aldrich (Taufkirchen, Germany). Methacrylic acid (stabilized), trehalose (for biochemistry), and dimethyl sulfoxide (for spectroscopy, Uvasol®) were obtained from Merck KgaA (Darmstadt, Germany). Ethyleneglycol dimethacrylate (98%, stabilized) and 2,2′-azobis(2-methylpropionitrile) (2,2′-Azobisisobutyronitrile = AIBN) (98%) were from Acros Organics, Geel, Belgium. RPMI-1640 w/o L-glutamine was purchased from Biowest S.A.S. (Nuaillé, France). Glutamine solution 200 mM and a solution of penicillin 10,000 U/mL and streptomycin 10,000 μg/mL were from BioWhittaker Europe (Verviers, Belgium). Polysorbate 80 (Tween 80) was obtained from ICI surfactants (Eversberg, Belgium) and Triton X-100 from Ferak (Berlin, Germany). Trypsine, FBS "Gold" and HBSS were from PAA Laboratories GmbH (Pasching, Austria).

2.1.1. Dimethacryloyl hydroxylamine

Dimethacryloyl hydroxylamine was prepared according to Yin et al. (2002). In brief, freshly distilled methacryloyl chloride (53 °C, 130 mbar) was added dropwise to a solution of hydroxylamine hydrochloride in pyridine and the mixture was stirred at 25–30 °C for 4 h. The reaction product was solved in chloroform, neutralized with HCl, and extracted three times with purified water. After drying with $MgSO_4$ and evaporation of the chloroform the oily product was solved in diethyl ether and crystallized by successive addition of n-heptane. The product was characterized by ^{1}H NMR, ^{13}C NMR, and mass spectroscopy:

^{1}H NMR ($CHCl_3$): ($C_8H_{11}NO_3$) δ = 1.9 [s, 3H, –N–CO–C(CH_3)=CH_2], 2.0 [s, 3H, –O–CO–C(CH_3)=CH_2], 5.4, 5.7 [s, 2H, –N–CO–C(CH_3)=CH_2], 5.8, 6.3 [s, 2H, –O–CO–C(CH_3)=CH_2], 9.3 [s, 1H, –CO–NH–O–]. ^{13}C NMR ($CHCl_3$): δ = 17.7 [s, –CO–C(CH_3)=CH_2], 122.0 [s, –N–CO–C(CH_3)=CH_2], 128.6 [s, –O–CO–C(CH_3)=CH_2], 133.1 [s, –O–CO–C(CH_3)=CH_2], 136.9 [s, –N–CO–C(CH_3)=CH_2], 165.7 [s, –N–CO–C(CH_3)=CH_2], 166.9 [s, –O–CO–C(CH_3)=CH_2]. Mass spectroscopy: 170 [H_2C=C(CH_3)–CO–NH_2–O–CO–C(CH_3)=CH_2]$^+$, 152 [H_2C=(C_4NO_2)–C(CH_3)=CH_2]$^+$, 87 [H_2C=C(CH_3)–C($OH)_2$]$^+$, 69 [H_2C=C(CH_3)–CHO]$^+$, 41 [H_2C=CH–CH_2]$^+$, 39 [HC≡C–CH_2]$^+$.

2.2. Preparation of particles

Polymerization was carried out in a 100 mL cylindrical laboratory reactor with a heating jacket and an anchor type stirrer (stirring rate 500 rpm). PVA and PEO-MA were solved in 25 mL water and a solution of MMA and the crosslinker in chloroform was added. After purging with nitrogen for 15 min the emulsion was heated to 65 °C and polymerization was started by adding a solution of AIBN in 2 mL chloroform. Stirring was continued for 8 h. Then the particles were separated by centrifugation, washed three times with water at 65 °C, and sonicated for 15 min to redisperge potential agglomerates.

2.3. Staining

A solution of DiI in toluene was added to the aqueous particle dispersion (40 μg DiI/mL) and vortexed for 5 min. The particles were isolated by centrifugation (10 min, 12,000 rpm) and washed with water. DiI loadings between 1.24 and 3.50 pg/μg were obtained.

2.4. Coating with polysorbate

A portion of each stained and unstained particle batch was coated with polysorbate 80 according to a procedure described by Sun et al. (2004). The particle dispersion was mixed with a polysorbate 80 stock solution to obtain a particle:polysorbate ratio of 1:1 and incubated at 2–6 °C for 24 h. One fraction of this particle dispersion was used in further experiments without removing excessive surfactant and the other fraction was washed with water by two cycles of centrifugation (10 min, 12,000 rpm) and redispersion with purified water.

2.5. Lyophilization

The suitability of PVA and trehalose as lyophilization stabilizers was tested in comparison to a batch free of excipients. Particles (as 0.1% dispersion) were mixed with 1.25% PVA or 5% trehalose, respectively and freeze dried in a Lyovac GT2 freeze-dryer (Finnaqua Santasalo-Sohleberg GmbH, Hürth, Germany) at −45 °C and 5.5×10^{-2} mbar (primary drying 15 h, secondary drying 20 °C, 2 h).

2.6. Particle size

The particle size was measured by photon correlation spectroscopy (PCS) using a ZetaPlus particle size analyzer (Brookhaven Instruments Corporation, Holtsville, NY, USA).

2.7. Zeta potential

Particles were isolated by centrifugation (10 min, 12,000 rpm) and resuspended in 10 mM tris buffer solution pH 7.4. The zeta potential was determined with a Zetasizer Nano ZS (Malvern Instruments Ltd., Malvern, UK) as the average of three measurements.

2.8. Electron microscopy

2.8.1. Transmission electron microscopy (TEM)

Samples were prepared for transmission electron microscopy (TEM) by negative staining. The sample suspension was dropped on a TEM grid and soaked up with filter paper after 30–60 s. Then a drop of uranyl acetate solution 2% (w/w) was pipetted on the grid and also soaked up after 30–60 s. Pictures were taken with a LEO CEM 902A EFTEM transmission electron microscope (Carl Zeiss SMT AG, Oberkochen, Germany) in the elastic bright field mode.

2.8.2. Scanning electron microscopy (SEM)

A drop of the particle suspension was dried on a coverslip, gold sputtered, and examined with a LEO-1450 VP scanning electron microscope (Carl Zeiss SMT AG, Oberkochen, Germany) (15 kV, magnification 4000×).

2.9. Particle degradation

0.1% particle suspensions were prepared with 0.1 M phosphate buffer solutions (pH 5.0, 7.4, and 9.0) and preserved with 0.02% sodium azide. The suspensions were filled into injection vials which were sealed, crimped and incubated in a reciprocating water bath at 37 °C. Samples were collected initially every 1–3 days, later on in larger intervals using a syringe with an injection needle. *Z*-average diameter and count rate of the undiluted samples were measured with a laser particle size analyzer (Zeta plus, Brookhaven Instruments Corp., Holtsville, NY, USA). Additionally sample droplets of the pH 9 degradation experiment were dried on coverslips, gold sputtered and SEM imaged as described above.

2.10. Cell culture

Mouse fibroblasts L929 (DSMZ, Braunschweig, Germany) were propagated as adherent culture in a medium containing 500 mL RPMI-1640, 5 mL glutamine solution 200 mM, 10 mL solution of penicillin 10,000 U/mL and streptomycin 10,000 μg/mL, and 50 mL FCS. Culture conditions were 37 °C, 5% CO_2, about 100% r.H., medium change intervals 2–3 days. Subcultivation: after sucking off the medium and two wash cycles with PBS the cells were detached with 0.25% trypsine solution at 37 °C. The process was stopped after 5 min by addition of culture medium, the cells were isolated by centrifugation (6 min, 300 × *g*) and resuspended in fresh medium.

2.11. Cell quantification

The viable cell count of the suspension was determined with a Neubauer counting chamber after 180 μL trypan blue solution 0.4% was added to a sample volume of 20 μL.

2.12. Determination of cellular particle uptake

Suspensions of DiI stained particles with concentrations of 100, 250, and 500 μg/mL were prepared and cellular particle uptake was studied using two different methods.

2.12.1. Fluorometry after cell lysis

20,000 cells per well were seeded in black 96 well cell culture microplates with flat clear bottom (Corning Life Sciences, Lowell, MA, USA) and cultivated for 2 days. When sufficient confluency was obtained the medium was sucked off and the wells were replenished with 90 μL HBSS buffer or with a 1:5 mixture of FCS and HBSS buffer. Subsequently 10 μL of the respective particle suspension was added and after homogenous mixing the plates were incubated on a shaker under the mentioned culture conditions. After the desired incubation time had elapsed the particle uptake was stopped and adherent particles were removed from the cells by triple rinsing with PBS. The fibroblasts were lysed by incubation (5 min, 37 °C) of the supernatant-free cell layer with a solution of 0.5% Triton X-100 in 0.2 N NaOH. The fluorescence intensity within the wells was measured with a FLUOstar OPTIMA plate reader (BMG LABTECH GmbH, Offenburg, Germany). All experiments were carried out in triplicate. For quantification of the DiI loading of stained particles 10 μL suspension of each particle batch and 90 μL water was transferred into a 96 well plate and the fluorescence intensity was measured as described before. A calibration function was determined from the fluorescence intensities of a dilution series of DiI in DMSO and used for both to calculate the DiI load of each particle suspension and to calculate the DiI uptake into the cells. From these two quantities the internalized portion of the initial particle mass was calculated. In order to estimate the number of incorporated particles, the incorporated particle mass was divided by the average mass of a single particle which can be calculated from the average particle diameter and the polymer density (1.19 g/cm^3), provided a spherical shape of the particles.

2.12.2. Flow cytometry

22,000 cells per well were seeded in 24 well cell culture plates and cultivated for 4 days. After confluency was achieved the supernatant was sucked off and replaced with 225 μL HBSS buffer or with a 1:5 mixture of FCS and HBSS buffer. Subsequently 25 μL of the respective particle suspension were added and after homogenous mixing the plates were incubated under the mentioned culture conditions. After the desired incubation time had elapsed non-incorporated particles were removed by sucking off the supernatant and washing the cells with 250 μL PBS. The cells were detached with 0.25% trypsine solution at 37 °C. The process was stopped after 5 min by addition of 450 μL culture medium. Until measurement the obtained cell suspension was stored in an ice bath. The cells were counted and analyzed with respect to their fluorescence caused by incorporated DiI using a flow cytometer COULTER® EPICS XL®-MCL™ with EXPO32 ADC software (Beckman Coulter, Inc., Fullerton, CA, USA). At 488 nm excitation the emitted fluorescence light was detected with the photomultiplier tube FL2 after passing a 575 nm bandpassfilter. All measurements were carried out in triplicate. Beside the cell samples incubated with stained particles a blank sample with untreated cells was analyzed. The mean value of each fluorescence intensity distribution was calculated and adjusted by subtracting the mean value of the untreated cells. Because of the differing DiI loads of the particle formulations and the fact that this method does not allow to measure cell-free reference samples the fluorescence intensities had to be normalized by the following calculation scheme: from the specific DiI loads measured fluorometrically after cell lysis as described above the ratios between the DiI content of each specific formulation and the DiI content of the least stained formulation were calculated. The adjusted mean value of each formulation's cytometric fluorescence intensity was divided by the respective DiI content ratio to obtain a directly comparable parameter quantifying the particle uptake.

2.13. Confocal laser scanning microscopy (CLSM)

About 100,000 cells were seeded on a collagen-coated circular coverslip inserted in a well of a 24 well cell culture plate. The collagen layer was applied by incubation of the coverslip with a 0.04% collagen solution (24 h, 37 °C) and subsequent drying in a laminar flow cabinet. After the cells were grown for 1 day the medium was removed and replaced by 450 μL fresh medium or HBSS buffer, respectively and 50 μL particle suspension. After 2 h the supernatant was sucked off and non-incorporated particles were removed by three wash cycles with PBS. 500 μL fixation solution, containing 3 g paraformaldehyde, 0.2 mL glutaraldehyde, 3.4 g sucrose per 100 mL PBS, were added. After 10 min the fixation solution was removed and the coverslip was placed cell-layered side down on a PVA coated microscope slide. Photomicrographs were made with a Zeiss LSM 510 CLSM.

2.14. Cytotoxicity tests

The cytotoxic potential of the particles was determined applying two methods.

2.14.1. CellTiter-Blue™ assay

4000 cells per well were seeded in black 96 well cell culture microplates with flat clear bottom (Corning Life Sciences, Lowell, MA, USA) and cultivated under the mentioned conditions. After 2 days the medium was replaced by 90 μL fresh medium, 10 μL particle suspension was added, homogenously

Table 1
Test formulations.

	Formulation no.				
	1 5% (w/w) DMHA	2 10% (w/w) DMHA	3 20% (w/w) DMHA	4 12% (w/w) EGDMA	5 8.5% (w/w) EGDMA 1.5% (w/w) MAA
Degree of crosslinking	3.8%	7.6%	15.2%	7.6%	5.3%
PEO-MA [g]	0.38	0.36	0.32	0.35	0.36
MMA [g]	1.52	1.44	1.28	1.41	1.44
DMHA [g]	0.10	0.20	0.40		
EGDMA [g]				0.24	0.17
MAA [g]					0.03
AIBN [g]	0.10	0.10	0.10	0.10	0.10
PVA [g]	0.10	0.10	0.10	0.10	0.10

mixed with the supernatant, and incubated 2 h before 20 μL CellTiter-Blue™ reagent (Promega Corporation, Madison, WI, USA) were added. The fluorescence intensity at 590 nm was determined after a residence time of 120 min with an excitation wavelength of 540 nm and expressed as a percentage related to the fluorescence measured without adding particle suspension to the cells. A sample of cells which were totally lysed with Triton X-100 served as positive control. A cell free mixture of reagent and culture medium was measured as a blank and also a mixture of reagent and particle suspension was tested to exclude possible interactions between the reagent and medium or particles.

2.14.2. ToxiLight® assay

4000 cells per well were seeded in black 96 well cell culture microplates with flat clear bottom (Corning Life Sciences, Lowell, MA, USA) and cultivated under the mentioned conditions. After 2 days the medium was replaced by 90 μL fresh medium. 10 μL particle suspension was added, homogenously mixed with the supernatant, and incubated 2 h before 20 μL of the supernatant were transferred into a well of a white microplate prefilled with 20 μL of the ToxiLight® reagent (Cambrex Corporation, East Rutherford, NJ, USA) and 100 μL PBS. After 5 min the luminescence intensity was measured with a FLUOstar OPTIMA plate reader at 22 °C (1 s integrated reading). The results were expressed as a percentage related to the luminescence of a sample which was totally lysed with the ToxiLight 100% Lysis Reagent. The test was also performed with cell-free medium and PBS.

3. Results and discussion

3.1. Formulations

Three particle formulations were prepared differing in type and amount of the cross-linker DMHA (Table 1). The total amount of monomers was 2.0 g in each formulation and the weight ratio PEO-MA/MMA equals 1:4. Beside these hydrolyzable particles a fourth formulation was prepared with the non-cleavable cross-linker EGDMA. The chosen ratio of 12% (w/w) EGDMA is equimolar to 10% (w/w) DMHA. Additionally a fifth formulation was prepared with 1.5% (w/w) methacrylic acid in order to study the influence of negatively charged monomers.

3.2. Particle size and shape

As can be seen from TEM and SEM images particles have a spherical shape, a smooth surface, and a diameter range between 150 and 1000 nm (Figs. 2 and 5a,e). *Z*-average diameters measured with PCS were 355 nm, 423 nm, 716 nm, 711 nm and 642 nm for formulations 1–5, respectively. The DMHA formulations reveal a positive correlation between the degree of cross-linking and the particle size. This might be explained with a stronger shrinkage of less cross-linked and thus less rigid particles when the better solvating chloroform is removed and replaced with the poorer solvating water (Scheler, 2007). Moreover, due to its hydrophilic nature DMHA improves the hydration of the polymer thus increasing particle porosity and size (Horák and Kroupová, 2004). Because of the larger spacing segment of EGDMA particles as big as those of formulation 3 are also obtained with the non-cleavable crosslinker even at a lower degree of crosslinking.

3.3. Freeze drying

To avoid structural changes lyophilization was chosen as a gentle method for drying the particles. Trehalose and PVA were tested as cryoprotectants. Suspensions of 0.1% particles in water or in solutions of 1.25% PVA, 5% trehalose or a mixture of 1.25% PVA and 5% trehalose were freeze dried at −45 °C for 15 h and final dried for 2 h at 20 °C. The periods of time necessary to disperse the dried products in water by gentle agitation of the vials were 10 s, >300 s, 9 s and 63 s, respectively (average of two measurements). PVA yields a gum-like xerogel which collapses upon contact with water forming a viscous clot which dissolves very slowly. In contrast particles stabilized with trehalose can be dispersed very easily within a few seconds. The intermediate value of a PVA/trehalose mixture shows that trehalose is also able to reduce the clumping effect of PVA. Products dried without any stabilizer can be also dispersed very rapidly but during the lyophilization process a large amount of the particles is lost as an aerosol. For this reason a scaffolding agent was found to be necessary for lyophilization of nanoparticles. Low molecular stabilizers like trehalose are favourable in terms of a rapid redispersion.

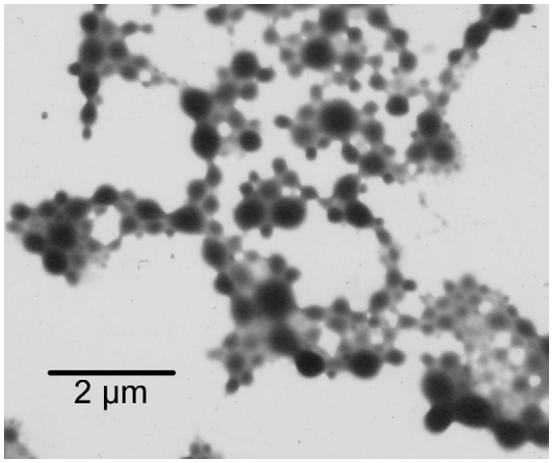

Fig. 2. TEM-photomicrograph of formulation 2.

Table 2
Zeta potential of test formulations.

	Formulation no.				
	1 5% (w/w) DMHA (mV)	2 10% (w/w) DMHA (mV)	3 20% (w/w) DMHA (mV)	4 12% (w/w) EGDMA (mV)	5 8.5% (w/w) EGDMA 1.5% (w/w) MAA (mV)
Uncoated	−13.1	−17.1	−16.6	−6.4	−16.8
Polysorbate 80-coated	−12.5	−12.2	−11.5	−3.9	–
Polysorbate 80-coated and washed	−12.9	−13.9	−13.0	−3.5	–

3.4. Zeta potential

Considering that DMHA is an easily hydrolysable molecule it can be assumed that a certain amount of free monomers or already polymerized DMHA is cleaved during the preparation process especially at the droplet or particle surface. Superficial carboxylic groups, created in this way, determine the zeta potential of the particles. As shown in Table 2 the least negative value was observed in particles cross-linked with the non-cleavable EGDMA. In the case of DMHA particles the negative potential increases when the degree of cross-linking rises from 3.8% to 7.6% and remains nearly constant up to 15.2% cross-linkage. The increase between 3.8% and 7.6% can be explained by the rising number of cleavable DMHA monomers, whereas the constant zeta potential at 15.2% cross-linkage might indicate a saturation of the particle surface with cleaved diacyl hydroxylamine units. Thus any further increase of DMHA in the formulation will not enhance the number of superficial carboxylic groups. To prove the hypothesis of free carboxylic groups, formed by cleaved diacyl hydroxylamine units, a cleavage of 30% of the hydrolysable linkages in formulation 2 was simulated by substitution of a corresponding amount of EGDMA in formulation 4 by MAA. The measured zeta potential was nearly the same as for formulations 2 and 3 thus confirming a cleavage of the cross linker during the preparation and giving evidence for a saturation of the particle surface with carboxylic groups. Though in the EGDMA/MAA formulation 5 a homogenous distribution of carboxylic groups within the whole polymer matrix has to be assumed it is likely that in the DMHA formulations the hydrolysis has taken place mainly at the particle surface. In these positions the diacyl hydroxylamine units are in contact with the aqueous medium over a more extended period of time than those which are sterically protected in the core of the particles. Thus it can be supposed that under these conditions the mentioned change of the zeta potential is caused by an overall degree of hydrolysis of even less than 30% of cross-linker. As can be seen from Table 2 the zeta potential was also influenced by adsorbed polysorbate. The particle charge decreased after adsorption of polysorbate and, except for formulation 4, increased again after washing. The negative charge of the particles is attenuated by the adsorbed surfactant layer (De Jaeghere et al., 2000). Peracchia et al. (1998) demonstrated that covalently bound PEG chains are able to reduce the zeta potential of cyanoacrylate nanoparticles from −30 mV even close to neutrality.

3.5. Particle degradation

The particle degradation was studied in dependence of cross-linkage (5%, 10% and 20% DMHA) and pH (5.0, 7.4 and 9.0) at 37 °C. EGDMA particles acted as a non-hydrolyzable reference. Freshly

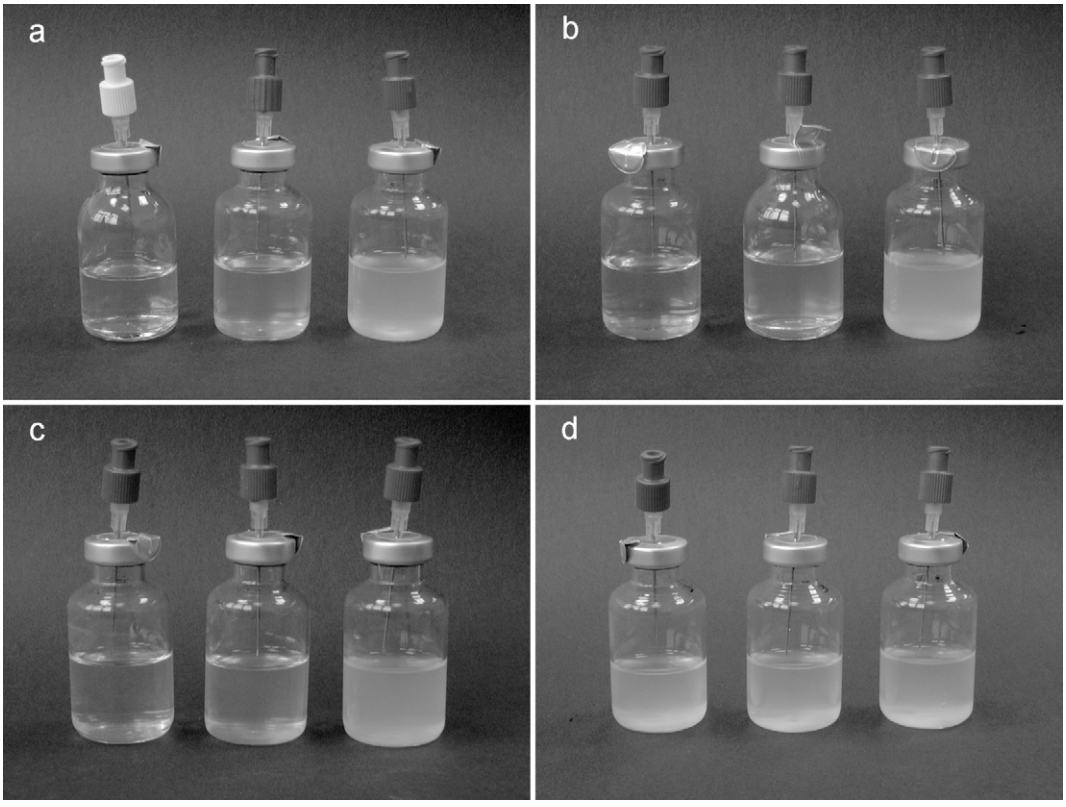

Fig. 3. Appearance of 0.1% particle solutions after 14 days incubation at 37 °C in different buffer solutions. Vials from left to right: pH 9.0, 7.4 and 5.0. (a) Formulation 1, (b) formulation 2, (c) formulation 3 and (d) formulation 4.

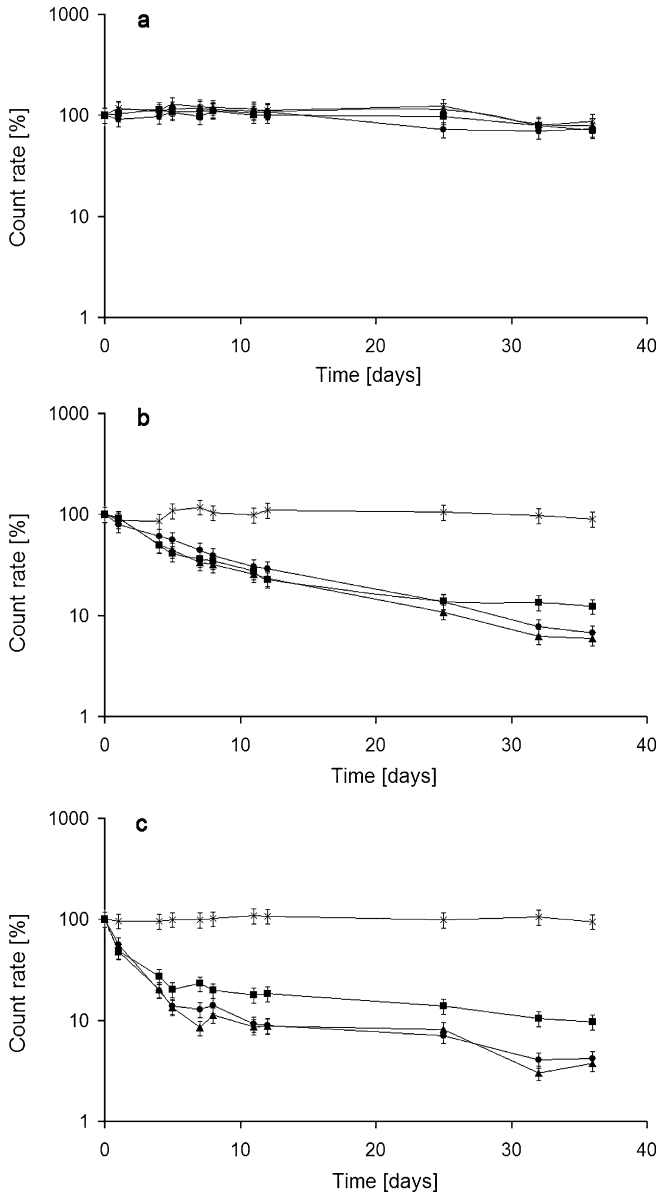

Fig. 4. Quantification of the disintegration process by dynamic light scattering:count rate vs. time profiles. (a) pH 5.0, (b) pH 7.4 and (c) pH 9.0. (●) Formulation 1, (▲) formulation 2, (■) formulation 3 and (×) formulation 4.

prepared dispersions of all tested particle formulations appeared turbid (Fig. 3). Only dispersions of EGDMA-cross-linked particles remained unchanged until the end of the test irrespective of the pH. Dispersions of DMHA particles with all degrees of cross-linkage became clear within 14 days at pH 9.0. At pH 7.4 only a very slight haze was left after 14 days incubation which seemed to be a little bit more pronounced at 20% cross-linkage. At pH 5.0, however, the turbidity remained completely unchanged in all formulations.

Dynamic light scattering (PCS) was chosen for quantifying the progress of particle degradation. Because of the wide size distribution of the initial particles which broadens further in the course of degradation the *Z*-average value turned out to be neither a significant nor a robust parameter for the description of the degradation profile. However the particle count was found to be discriminative and suitable to clearly illustrate differences in the degradation pattern. Fig. 4 shows the count rate vs. time profiles of the tested formulations with the count rate given in percent of the initial value. Particles cross-linked with EGDMA did not show significant degradation at any pH. At pH 5.0 also the DMHA particles were stable over the whole test period of 35 days. By contrast at pH 7.4 and pH 9.0 the count rate decreased following a first order kinetics in the initial phase. At pH 7.4 the degree of cross-linking did not have any significant influence on the degradation rate. The initial degradation rate at pH 9.0 was higher than at pH 7.4 for all tested degrees of cross-linking. The profiles of the lower cross-linked preparations 1 and 2 (5% and 10% DMHA) did not show any significant difference whereas the higher cross-linked formulation 3 degraded clearly slower. Differences of the kinetics occurred mainly within the first 5 days. Then the degradation proceeded with almost the same lower rate for all preparations.

The morphological changes of the particles during incubation at pH 9.0 are illustrated in Fig. 5a–h. Due to the cleavage of the cross-linkages the particles with 10% DMHA (formulation 2) became less rigid, developed a gel-like, softened structure and spread when they were dried on the surface of a coverslip. After already four days the particles had become sufficiently ductile to lose their spherical shapes and blend into each other during SEM preparation. After 17 days most of the remaining particles had coalesced and formed conglomerates with blurred outlines. In contrast EGDMA particles did not show any morphological change and maintained their spherical shape during the whole test period of 17 days.

3.6. Cellular particle uptake

The uptake of uncoated and polysorbate coated particles into L929 mouse fibroblasts was investigated by flow cytometry. For this method does not allow to determine the absolute mass of internalized particles a bridging study was made with a subset of samples to correlate the results of the cytometric method with those of fluorometry after cell lysis. With the regression function of these data all further flow cytometric results were converted to indicate the particle uptake in pg/cell.

The cells were incubated for 1, 2, and 4 h with particle suspensions of three different concentrations (10, 25 and 50 μg/mL). The particle uptake did not show any saturation within the experimental range up to 50 μg/mL (Fig. 6). In the literature a dose-dependent uptake is described for various kinds of nanoparticles and different cell types (Foged et al., 2005; Vasir and Labhasetwar, 2007; Chavanpatil et al., 2007). For poly(lactide-co-glycolide) nanoparticles and human vascular smooth muscle cells Panyam and Labhasetwar (2003) found a linear relationship within the concentration range from 10 to 100 μg/mL followed by a reduced uptake efficiency at higher doses from 500 to 1000 μg/mL. Proportionality was also reported for the uptake of polylactic acid nanoparticles into retinal pigment epithelial cells covering the concentration range up to 1000 μg/mL (Bejjani et al., 2005). The reported numbers of particles internalized per cell (9.8 at 10 μg/mL, 22.2 at 100 μg/mL, and 218 μg/mL at 1000 μg/mL within 6 h) are lower than in our experiments in which values between 2.9 and 35.3 (incubation with 10 μg particles/mL) and between 11.2 and 272.7 (50 μg particles/mL) were already reached within 2 h.

Within the tested range from 1 to 4 h also a linear correlation between particle uptake and incubation time could be demonstrated (Fig. 7). A time dependency of particle internalization is frequently described for a variety of particles and cell types (Bejjani et al., 2005; Harush-Frenkel et al., 2007; Nakano et al., 2007; Panyam and Labhasetwar, 2003; Chavanpatil et al., 2007). Saturation is often achieved after 4–6 h but in other cases the particle uptake continues for over 24 h (Mailänder and Landfester, 2009). The strict linearity over 4 h in our study indicates a slow process with a late onset of saturation. For a receptor mediated internalization is usually much faster than an unspecific uptake probably the studied process takes place without any receptor involvement.

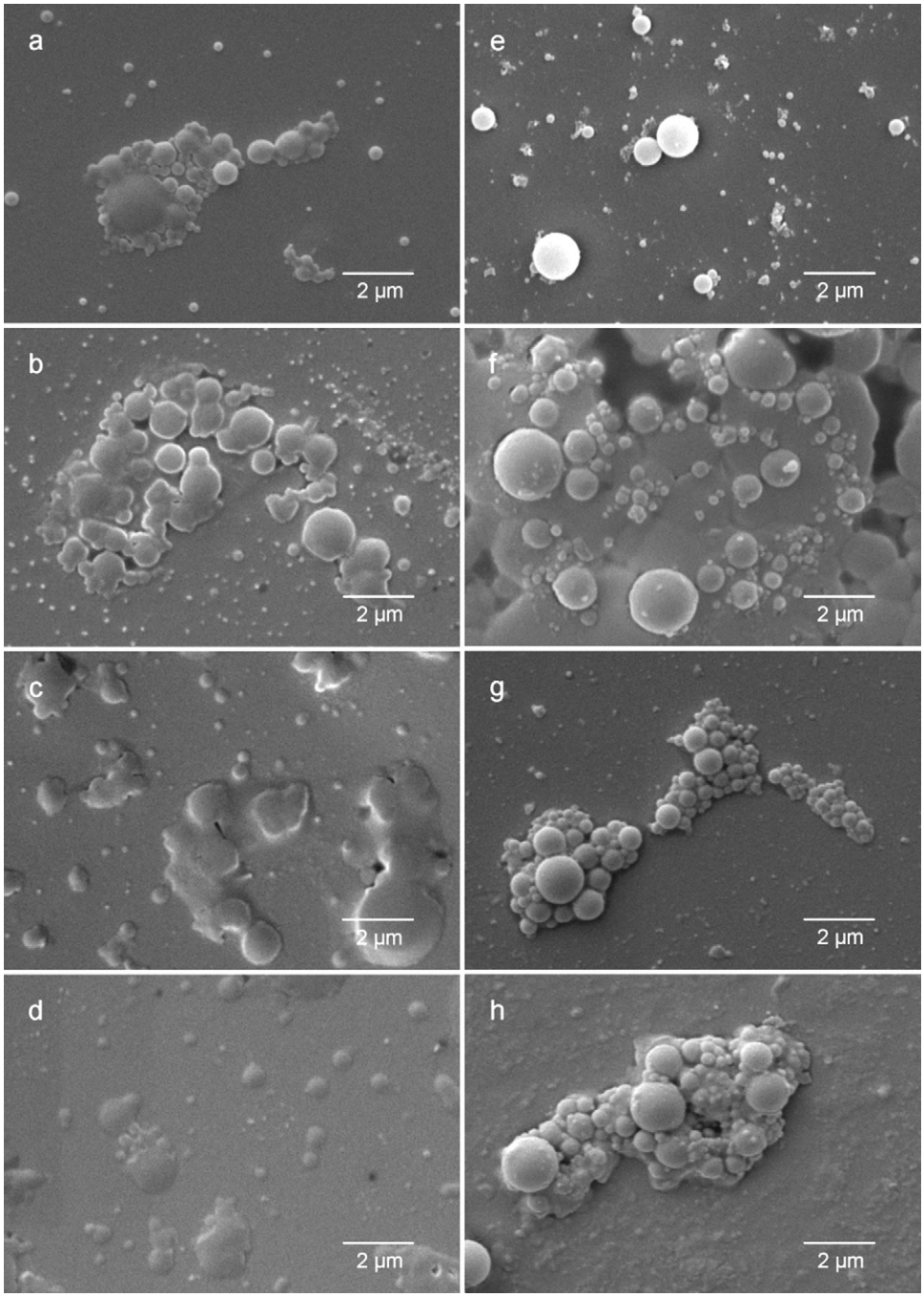

Fig. 5. SEM photomicrographs of the particle disintegration process at pH 9.0 after 0, 4, 11 and 17 days (from top to down). (a)–(d) Formulation 2; (e)–(h) formulation 4.

The uptake of the tested formulations increased in the order 2 (10% DMHA) < 5 (EGDMA/MAA) < 3 (20% DMHA) < 1 (5% DMHA) < 4 (EGDMA). The main parameter to explain the inter-formulation differences is the particle charge measured as the zeta potential. In order to illustrate this influence, the rate of particle uptake was calculated as the slope of each regression line in a particle uptake vs. time diagram. Fig. 8 shows a strong linear correlation between the rate of particle uptake and zeta potential for different times of incubation. As could be shown by multivariate regression analysis a second but weaker factor of influence was the particle size. Its effect was limited to the first 2 h of incubation and vanished after 4 h. Among all factors controlling the particle uptake the particles' surface properties, including the surface charge, are considered to be most important and their influence is often more significant than that of the particle size (Chen et al., 2009; Huang et al., 2004). The following correlation was found to describe the average mass of internalized particles per cell m_i [pg/cell] at a concentration of 25 µg/mL in dependence of incubation time t [h], zeta potential ζ [mV], and particle diameter d [nm]:

$$m_i = -2.16 + 5.03t - 1.03 \times 10^{-2}\zeta + 3.92 \times 10^{-3}d + 2.33 \times 10^{-1}t\zeta - 6.98 \times 10^{-4}td + 6.59 \times 10^{-5}\zeta d$$

The zeta potential showed a continuous correlation only with the weight but not with the number of internalized particles. Remarkably, the particle uptake decreased when the surface charge becomes more negative. This is in contrast to the widely held view

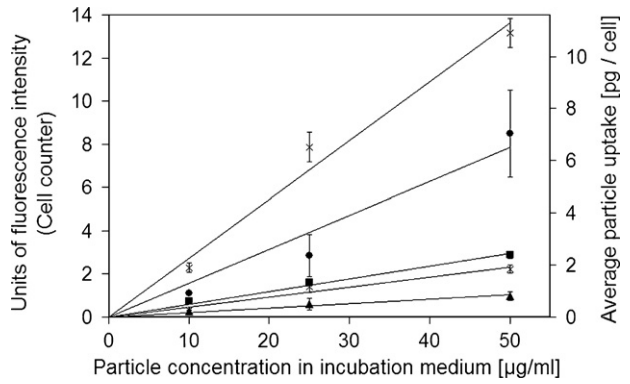

Fig. 6. Cellular particle uptake by mouse fibroblasts (L929): dependence on particle concentration in the incubation medium after 2 h incubation: (●) formulation 1, (▲) formulation 2, (■) formulation 3, (×) formulation 4 and (*) formulation 5.

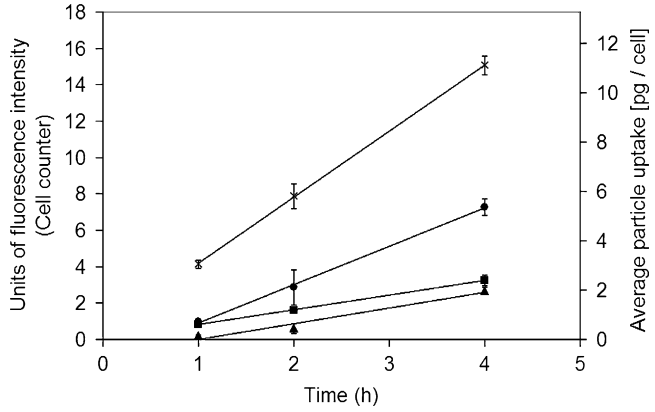

Fig. 7. Cellular particle uptake by mouse fibroblasts (L929): dependence on incubation time: (●) formulation 1, (▲) formulation 2, (■) formulation 3 and (×) formulation 4 (25 µg/mL).

that cationic or anionic particles are internalized more rapidly than neutral particles (Harush-Frenkel et al., 2007; Dobrovolskaia and McNail, 2007; Patil et al., 2007; Wilhelm et al., 2003). However there is also evidence for an inhibitory effect of higher densities of negative charges. The uptake of poly(styrene-co-acrylic acid) nanoparticles by HeLa cells showed an optimum at a COOH-density of around 0.5 superficial carboxylic groups per nm^2 and a decrease at higher densities (Mailänder and Landfester, 2009; Holzapfel et al., 2005). About the same density of dicarbonyl hydroxylamine

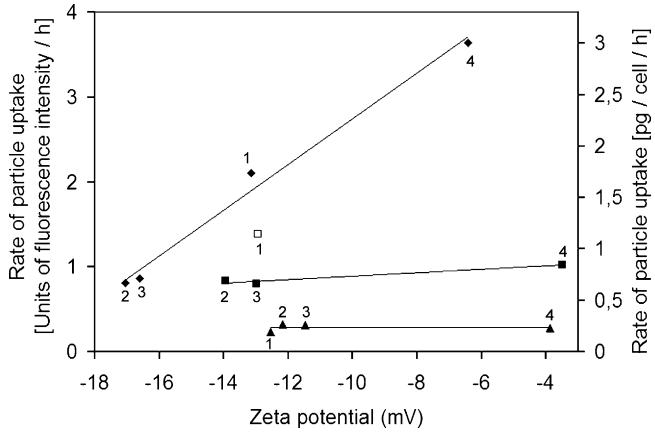

Fig. 8. Rate of cellular particle uptake: dependence on zeta potential. Formulations 1–4 (♦) without polysorbate coating, (▲) coated with polysorbate 80 and (■) coated with polysorbate 80 and subsequently washed (25 mg/mL).

groups could be estimated for the lowest crosslinked formulation 1 by stereochemical considerations using ACD/ChemSketch Freeware (version 10.00, Advanced Chemistry Development, Inc., Toronto, ON, Canada, www.acdlabs.com, 2006). It can be presumed that hydrolysis which should take place most rapidly at the particle surface converts the major part of those cleavable linkages into carboxylic groups even during the preparation process. Therefore their superficial density in the tested formulations ranges most likely from about 0.5 nm^{-2} to higher values and increases in parallel with the degree of crosslinking. Thus, the only slightly negative surface of the non-cleavable or low DMHA-crosslinked particles provides better conditions for cellular uptake whereas a higher density of negative charges impedes their internalization.

If the particles were coated with polysorbate the internalization rate dropped close to zero and the charge dependence disappeared (Fig. 8). Because of their surface-active nature polysorbate molecules adhere to the particle surface and cover them with further PEG chains. As discussed before, this changes the zeta potential to less negative values. As a result the particle uptake should increase but surprisingly the opposite happens, which indicates that the polysorbate coating acts by another effect apart from decreasing the negative zeta potential.

Numerous studies describe that coating of nanoparticles with polysorbate facilitates a specific, receptor mediated endocytosis and furthermore enables the particles to pass the blood–brain-barrier by a transcytotic mechanism (Kim et al., 2007, Ramge et al., 2000; Kreuter, 2001; Borchard et al., 1994). Polysorbate plays the role of an anchor mediating the adsorption of ApoE and ApoB from the plasma. This facilitates the particles to interact with the LDL receptor on the cell membrane leading to their uptake by an endocytic process. Although the LDL receptor could be detected on L929 mouse fibroblasts specific uptake of polysorbate coated particles was not to be expected in those experiments which were performed with serum free incubation medium.

Addition of 20% FCS did not increase the particle uptake significantly but decreased it in most cases in some of them even by half, providing further evidence for a non-specific uptake mechanism. A probable reason for this reduction is the fact that the exocytosis of internalized particles is inhibited in serum-free media and becomes active again after addition of FCS (Panyam and Labhasetwar, 2003).

L929 mouse fibroblasts are non-phagocytic cells (Li et al., 2008; Ghigo et al., 2008; Harley et al., 1998). According to a prevailing view the upper limit of the size of nanoparticles internalized into non-phagocytotic cells by non-specific endocytosis is 150 nm but also the internalization of particles up to 3 µm is reported (Conner and Schmid, 2003; Gary et al., 2007; Oupicky et al., 2000; Gratton et al., 2008a,b; Park and Cho, 2007). A higher cut-off size than 150 nm also applies to mouse fibroblasts as shown by Olivier et al. (2003) who reported the uptake of 450 nm polystyrene particles by L929 cells. By means of confocal laser scanning microscopy we could prove that the particles despite their size of up to 716 nm did not adhere to the membrane but were actually internalized by the cells (Fig. 9).

3.7. Cytotoxicity

Cell metabolism and membrane integrity after particle incubation was studied with the CellTiter Blue and the ToxiLight assay, respectively. The CellTiter Blue assay is based on the reductive conversion of resazurine to the fluorescent resurofine which can only be accomplished by metabolically active cells. Incubation with nanoparticles increased the fluorescence of all samples in comparision to cells treated with particle free medium. This indicates the absence of metabolic cytotoxicity and, what is more remarkable, it even demonstrates an activation of the cell metabolism. Testing human fibroblasts (hTERT-BJ1) upon incubation with crosslinked

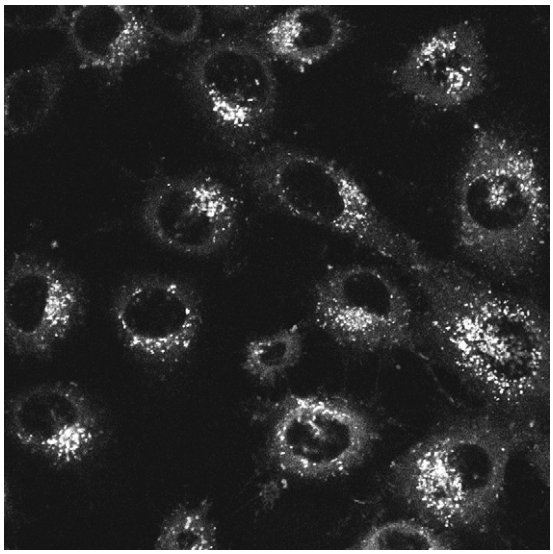

Fig. 9. Confocal laser scanning photomicrograph of L929 mouse fibroblasts with internalized nanoparticles after 2 h incubation with formulation 1 (25 μg/mL).

gelatin nanoparticles using the MTT assay Gupta et al. (2004) also found an increase of cell metabolism up to 120–140%. As Fig. 10 shows, this activation exhibited a similar correlation to the particles' zeta potential as was found for the uptake of surfactant free particles into the cells. This suggests that the particle internalization stimulates the cell metabolism. Interestingly the metabolic stimulation caused by polysorbate coated and uncoated particles is about the same even though polysorbate coating decreases the intracellular particle accumulation. It seems unlikely that metabolic processes are activated by nanoparticles outside the cells especially if they have no specific binding structures. As a hypothesis, coated and uncoated particles might enter the cell to about the same extent by unspecific endocytosis and/or macropinocytosis thereby boosting the metabolism but coated particles are exocytosed much more readily. This would explain the equal metabolic stimulation by both types of particles despite of their different intracellular accumulation. It is well known that external material is internalized through early endocytotic vesicles and trafficked to sorting endosomes which, depending on the signals presented by the material, recycle them back to the outside of the cell or convey them to other cellular organelles (Chavanpatil et al., 2007). A major fraction, up to 85% of endocytosed particles undergoes subsequent exocytosis with larger or aggregated particles are less likely to be

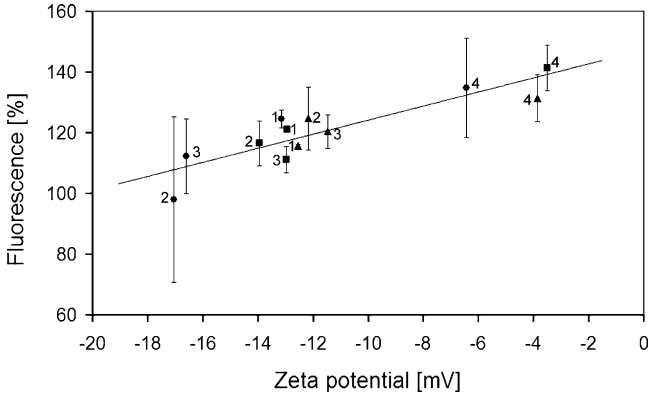

Fig. 10. Dependence of metabolic activity (% fluorescence measured with the CellTiter Blue assay) on the zeta potential after 2 h incubation (25 μg/mL). Formulations 1–4 (♦) without polysorbate coating, (▲) coated with polysorbate 80 and (■) coated with polysorbate 80 and subsequently washed.

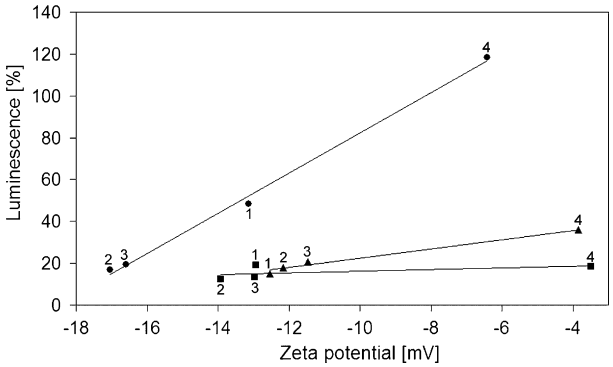

Fig. 11. Dependence of membrane integrity (% luminescence measured with the ToxiLight assay) on the zeta potential after 2 h incubation (10 μg/mL). Formulations 1–4 (♦) without polysorbate coating, (▲) coated with polysorbate 80 and (■) coated with polysorbate 80 and subsequently washed.

exocytosed than smaller ones (Sahoo and Labhasetwar, 2005; Jin et al., 2008; Chithrani and Chan, 2007). Thus exocytosis has to be regarded as an important obstacle for the transfer of nanoparticles into cells and should always be considered as a possible reason if nanoparticles fail to be delivered into cells (Park and Cho, 2007).

The integrity of the cell membrane was measured by the ToxiLight test. This is a non-destructive assay which quantifies the release of adenylate kinase (AK) from damaged cells. AK in the culture medium converts ADP to ATP which subsequently reacts with luciferin. The intensity of the light which is emitted during this luciferase-catalyzed reaction is linearly related to the AK concentration. For polysorbate-free particles a linear correlation between the zeta potential and the luminescence intensity was found (Fig. 11). This indicates a damage of the cell membrane corresponding to the amount of internalized particles. Polysorbate coated particles cause only little AK release. Likewise, they accumulate intracellularly only to a very limited extent. Thus it seems that membrane damage is caused mainly by those particles which are actually deposited in the cells. A correlation between particle uptake and cell damage was also described by other investigators (Hong et al., 2006). Fröhlich et al. (2009), for example, found that 20 nm carboxylated polystyrene nanoparticles, which were cytotoxic, were internalized to a higher degree than 200 nm ones, which were not cytotoxic. Remarkably they could not detect the membrane damage by the AK release (ToxiLight assay) while some other tests worked.

4. Conclusion

The diacyl hydroxylamine group provides a hydrolytically cleavable moiety for the synthesis of biodegradable crosslinked polymers. We could demonstrate that nanoparticles made of such polymers have the potential to be used as drug carriers for intracellular delivery. Poly(ethylene glycol-graft-methyl methacrylate) nanoparticles crosslinked with dimethacryloyl hydroxylamine degrade within the neutral and alkaline pH range but are stable under acidic conditions (pH 5). This is in contrast to widely used PLA and PLGA particles for which degradation increases in acidic media. In terms of use, nanoparticles made of DMHA-crosslinked polymers should be able to withstand the acidic environment within lysosomes (pH 4.8) and to release encapsulated drug not before the particles have reached the neutral cytoplasm (pH 7.2). All tested particles entered L929 mouse fibroblasts in a concentration and time dependent manner. The zeta potential was found to be the main factor of influence for the uptake rate whereas the particle size plays only a minor role. The particle internalization increased as the zeta potential decreased from −17 to −6 mV. Coating with polysor-

bate 80 impaired the particle uptake and abolished its dependence on the zeta potential. A similar pattern of correlation with the zeta potential was also found for the degree of membrane damage, thus suggesting that the intracellularly accumulated particles compromise the membrane integrity. The metabolic activity, by contrast, rose as the surface charge became less negative without any additional influence of polysorbate coating. As for coated particles did hardly accumulate within the cells, metabolic stimulation was assumed to be either triggered upon membrane contact of the particles or upon endocytosis via early endosomes followed by selective exocytosis of the coated particle fraction. Addition of 20% FCS decreased the particle uptake most probably due to an increased exocytosis.

Acknowledgements

The authors gratefully acknowledge the assistance received from Mrs. K. Greiner, Mrs. R. Kaiser (EMZ Jena) and Mrs. I. Lehmann in the preparation of the TEM, SEM and CLSM photomicrographs. Our thanks are also extended to Mrs. A. Herre and Mrs. R. Brabetz for their support in cell culture.

References

Bejjani, R.A., BenEzra, D., Cohen, H., Rieger, J., Andrieu, C., Jeanny, J.C., Golomb, G., Behar-Cohen, F.F., 2005. Nanoparticles for gene delivery to retinal pigment epithelial cells. Mol. Vis. 11, 124–132.

Borchard, G., Audus, K.L., Shi, F., Kreuter, J., 1994. Uptake of surfactant-coated poly(methymethacrylate)-nanoparticles by bovine brain microvessel endothelial cell monolayers. Int. J. Pharm. 110, 29–35.

Calvo, J.P., Gouritin, B., Chacun, H., Desmaële, D., D'Angelo, J., Noel, J.P., Georgin, D., Fattal, E., Andreux, J.P., Couvreur, P., 2001. Long-circulating PEGylated polycyanoacrylate nanoparticles as new drug carrier for brain delivery. Pharm. Res. 18, 1157–1166.

Chavanpatil, M.D., Khdair, A., Panyam, J., 2007. Surfactant–polymer nanoparticles: a novel platform for sustained and enhanced cellular delivery of water-soluble molecules. Pharm. Res. 24, 803–810.

Chen, Z.P., Xu, R.Z., Zhang, Y., Gu, N., 2009. Effects of proteins from culture medium on surface property of silans-functionalized magnetic nanoparticles. Nanoscale Res. Lett. 4, 204–209.

Chithrani, B.D., Chan, W.C.W., 2007. Elucidating the mechanism of cellular uptake and removal of protein-coated gold nanoparticles of different sizes and shapes. Nano Lett. 7, 1542–1550.

Chivukula, P., Dusek, K., Wang, D., Dusková-Smrcková, M., Kopecková, P., Kopeček, J., 2006. Synthesis and characterization of novel aromatic azo bond-containing pH-sensitive and hydrolytically cleavable IPN hydrogels. Biomaterials 27, 1140–1151.

Conner, S.D., Schmid, S.L., 2003. Regulated portals of entry into the cell. Nature 422, 37–44.

De Jaeghere, F., Allemann, E., Feijen, J., Kissel, T., Doelker, E., Gurny, R., 2000. Cellular uptake of PEO surface-modified nanoparticles: evaluation of nanoparticles made of PLA:PEO diblock and triblock copolymers. J. Drug Target 8, 143–153.

Dobrovolskaia, M.A., McNail, S.E., 2007. Immunological properties of engineered nanomaterials. Nat. Nanotechnol. 2, 469–478.

Foged, C., Brodin, B., Frokjaer, S., Sundblad, A., 2005. Particle size and surface charge affect particle uptake by human dendritic cells in an in vitro model. Int. J. Pharm. 298, 315–322.

Fröhlich, E., Samberger, C., Kueznik, T., Absenger, M., Roblegg, E., Zimmer, A., Pieber, T.R., 2009. Cytotoxicity of nanoparticles independent from oxidative stress. J. Toxicol. Sci. 34, 363–375.

Gary, D.J., Puri, N., Won, Y.Y., 2007. Polymer-based siRNA delivery: perspectives on the fundamental and phenomenological distinctions from polymer-based DNA delivery. J. Control. Release 121, 64–73.

Ghigo, E., Kartenbeck, J., Lien, P., Pelkmans, L., Capo, C., Mege, J.L., Raoult, D., 2008. Ameobal pathogen mimivirus infects macrophages through phagocytosis. PLoS Pathog. 4, e1000087.

Gratton, S.E.A., Ropp, P.A., Pohlhaus, P.D., Luft, J.C., Madden, V.J., Napier, M.E., DeSimone, J.M., 2008a. The effect of particle design on cellular internalization pathways. PNAS 105, 11613–11618.

Gratton, S.E.A., Napier, M.E., Ropp, P.A., Tian, S., DeSimone, J.M., 2008b. Microfabricated particles for engineered drug therapies: elucidation into the mechanisms of cellular internalization of PRINT particles. Pharm. Res. 25, 2845–2852.

Gupta, A.K., Gupta, M., Yarwood, S.J., Curtis, A.S.G., 2004. Effect of cellular uptake of gelatin nanoparticles on adhesion, morphology and cytoskeleton organisation of human fibroblasts. J. Control. Release 95, 197–207.

Harley, V.S., Dance, D.A., Drasar, B.S., Tovey, G., 1998. Effects of *Burkholderia pseudomallei* and other Burkholderia species on eukaryotic cells in tissue culture. Microbios 96, 71–93.

Harush-Frenkel, O., Debotton, N., Benita, S., Altschuler, Y., 2007. Targeting of nanoparticles to the clathrin-mediated endocytic pathway. Biochem. Biophys. Res. Commun. 353, 26–32.

Holzapfel, V., Musyanovych, A., Landfester, K., Lorenz, M.R., Mailänder, V., 2005. Preparation of fluorescent carboxyl and amino functionalized polystyrene particles by miniemulsion polymerization as markers for cells. Macromol. Chem. Phys. 206, 2440–2449.

Hong, S., Hessler, J.A., Banaszak Holl, M.M., Leroueil, P.R., Mecke, A., Orr, B.G., 2006. Physical interactions of nanoparticles with biological membranes: the observation of nanoscale hole formation. J. Chem. Health Saf. 13, 16–20.

Horák, D., Chaykivskyy, O., 2002. Poly(2-hydroxyethyl methacrylate-co-N,O-dimethacryloylhydroxylamine) particles by dispersion polymerization. J. Polym. Sci. A 40, 1625–1632.

Horák, D., Kroupová, J., Šlouf, M., Dvořák, P., 2004. Poly(2-hydroxyethyl methacrylate)-based slabs as a mouse embryonic stem cell support. Biomaterials 25, 5249–5260.

Huang, M., Khor, E., Lim, L.Y., 2004. Uptake and cytotoxicity of chitosan molecules and nanoparticles: effects of molecular weight and degree of deacetylation. Pharm. Res. 21, 344–353.

Jin, H., Heller, D.A., Strano, M.S., 2008. Single-particle tracking of endocytosis and exocytosis of single-walled carbon nanotubes in NIH-3T3 cells. Nano Lett. 8, 1577–1585.

Kim, H.R., Andrieux, G.K., Nicolas, V., Appel, M., Chacum, H., Desmaële, D., Taran, F., Georgin, D., Couvreur, P., 2007. Low-density lipoprotein receptor-mediated endocytosis of PEGylated nanoparticles in rat brain endothelial cells. Cell. Mol. Life Sci. 64, 356–364.

Kreuter, J., 2001. Nanoparticulate systems for brain delivery of drugs. Adv. Drug Deliv. Rev. 47, 65–81.

Li, L., Li, X., Yan, J., 2008. Alterations of concentrations of calcium and arachidonic acid and agglutinations of microfilaments in host cells during *Toxoplasma gondii* invasion. Vet. Parasitol. 157, 21–33.

Mailänder, V., Landfester, K., 2009. Interaction of nanoparticles with cells. Biomacromolecules 10, 2379–2400.

Nakano, K., Bando, Y., Tozuka, Y., Takeuchi, H., 2007. Cellular interaction of PEGylated PLGA nanospheres with macrophage J774 cells using flow cytometry. Asian J. Pharm. Sci. 2, 220–226.

Olivier, V., Duval, J.L., Hindié, M., Pouletaut, P., Nagel, M.D., 2003. Comparative particle-induced cytotoxicity toward macrophages and fibroblasts. Cell. Biol. Toxicol. 19, 145–159.

Oupicky, D., Konak, C., Ulbrich, K., Wolfert, M.A., Seymour, L.W., 2000. DNA delivery systems based on complexes of DNA with synthetic polycations and their copolymers. J. Control. Release 65, 149–171.

Panyam, J., Labhasetwar, V., 2003. Dynamics of endocytosis and exocytosis of poly(D,L-lactide-co-glycolide) nanoparticles in vascular smooth muscle cells. Pharm. Res. 20, 212–220.

Park, J.S., Cho, Y.W., 2007. In vitro cellular uptake and cytotoxicity of paclitaxel-loaded glycol chitosan self-assembled nanoparticles. Macromol. Res. 15, 513–519.

Patil, S., Sandberg, A., Heckert, E., Self, W., Seal, S., 2007. Protein adsorption and cellular uptake of cerium oxide nanoparticles as a function of zeta potential. Biomaterials 28, 4600–4607.

Peracchia, M.T., Vauthier, C., Desmaële, D., Gulik, A., Dedieu, J.C., Demoy, M., D'Angelo, J., Couvreur, P., 1998. Pegylated nanoparticles from a novel methoxypolyethylene glycol cyanoacrylate–hexadecyl cyanoacrylate amphiphilic copolymer. Pharm. Res. 15, 550–556.

Přádný, M., Michálek, J., Lesný, P., Hejčl, J., Šlouf, M., Syková, E., 2006. Macroporous hydrogels based on 2-hydroxyethylmethacrylate, Part 5: hydrolytically degradable materials. J. Mater. Sci. Mater. Med. 17, 1357–1364.

Ramge, P., Unger, R.E., Oltrogge, J.B., Zenker, D., Begley, D., Kreuter, J., von Briesen, H., 2000. Polysorbate-80 coating enhances uptake of polybutylcyanoacrylate (PBCA)-nanoparticles by human and bovine primary brain capillary endothelial cells. Eur. J. Neurosci. 12, 1931–1940.

Rosen, H., Kohn, J., Leong, K., Langer, R., 1988. Bioerodible polymers for controlled release systems. In: Hsieh, D. (Ed.), Controlled Release Systems: Fabrication Technology. CRC Press, Boca Raton, pp. 83–110.

Sahoo, S.K., Panyam, J., Prabha, S., Labhasetwar, V., 2002. Residual polyvinyl alcohol associated with poly (D,L-lactide-coglycolide) nanoparticles affects their physical properties and cellular uptake. J. Control. Release 82, 105–114.

Sahoo, S.K., Labhasetwar, V., 2005. Enhanced antiproliferative activity of transferrin-conjugated paclitaxel-loaded nanoparticles is mediated via sustained intracellular drug retention. Mol. Pharm. 2, 373–383.

Scheler, S., 2007. A novel approach to the interpretation and prediction of solvent effects in the synthesis of macroporous polymers. J. Appl. Polym. Sci. 105, 3121–3131.

Smith, M.H., South, A.B., Gaulding, J.C., Jyon, L.A., 2010. Monitoring the erosion of hydrolytically-degradable nanogels via multiangle light scattering coupled to asymmetrical flow field–flow fractionation. Anal. Chem. 82, 523–530.

Šubr, V., Duncan, R., Kopeček, J., 1990. Release of macromolecules and daunomycin from hydrophilic gels containing enzymatically degradable bonds. J. Biomater. Sci. Polym. 4, 261–278.

Sun, W., Xie, C., Wang, H., Hu, Y., 2004. Specific role of polysorbate 80 coating on the targeting of nanoparticles to the brain. Biomaterials 25, 3065–3071.

Syková, E., Jendelová, P., Urdzíková, L., Lesný, P., Hejčl, J., 2006. Bone marrow stem cells and polymer hydrogels—two strategies for spinal cord injury repair. Cell. Mol. Neurobiol 26, 1111–1127.

Ulbrich, K., Strohalm, J., Kopeček, J., 1982. Polymers containing enzymatically degradable bonds VI. Hydrophilic gels cleavable by chymotrypsin. Biomaterials 3, 150–154.
Ulbrich, K., Šubr, V., Seymour, L.W., Duncan, R., 1993. Novel biodegradable hydrogels prepared using divinylic crosslinking agent N,O-dimethacryloylhydroxylamine, 1. Synthesis and characterisation of rates of gel degradation, and rate of release of model drugs, in vitro and in vivo. J. Control. Release 24, 181–190.
Vasir, J.K., Labhasetwar, V., 2007. Biodegradable nanoparticles for cytosolic delivery of therapeutics. Adv. Drug Deliv. Rev. 59, 718–728.
Wilhelm, C., Billotey, C., Roger, J., Pons, J.N., Bacri, J.C., Gazeau, F., 2003. Intracellular uptake of anionic superparamagnetic nanoparticles as a function of their surface coating. Biomaterials 24, 1001–1011.
Yin, W., Akala, E.O., Taylor, R.E., 2002. Design of naltrexone-loaded hydrolyzable crosslinked nanoparticles. Int. J. Pharm. 244, 9–19.